Appl Phys A (2010) 100: 1109–1114
DOI 10.1007/s00339-010-5711-3

Applied Physics A
Materials Science & Processing

Thermoelectric properties of *n*-type $\mathrm{Sr}_x M_y \mathrm{Co_4Sb_{12}}$ ($M = \mathrm{Yb, Ba}$) double-filled skutterudites

S.Q. Bai · X.Y. Huang · L.D. Chen · W. Zhang · X.Y. Zhao · Y.F. Zhou

Received: 12 August 2009 / Accepted: 2 November 2009 / Published online: 4 May 2010

Abstract Alkaline-earth (AE) and rare-earth (RE) atoms are usually used as void fillers in the caged compound $CoSb_3$ to improve the thermoelectric performance of the filled system. Polycrystalline single-filled $Sr_{0.21}Co_4Sb_{12}$, double-filled $Sr_xYb_yCo_4Sb_{12}$, and $Sr_xBa_yCo_4Sb_{12}$ skutterudites have been synthesized. Rietveld structure refinement confirms that both Sr and Yb occupy the Sb-icosaedron voids in skutterudite frame work. In this paper, we report the high-temperature thermoelectric properties including electrical conductivity, Seebeck coefficient, and thermal conductivity. Double filling of the Sr–Yb combinations shows a stronger suppression on lattice thermal conductivity than that of Sr–Ba combination. Furthermore, the double-filled $Sr_xYb_yCo_4Sb_{12}$ skutterudites exhibit a much higher power factor than the Sr-filled system. The maximum power factor for $Sr_{0.22}Yb_{0.03}Co_4Sb_{12.12}$ reaches 41 $\mu W\,cm^{-1}\,K^{-2}$ at room temperature and 57.5 $\mu W\,cm^{-1}\,K^{-2}$ at 850 K, respectively. The enhanced thermoelectric figures of merit are 1.32 for $Sr_xYb_yCo_4Sb_{12}$ and 1.22 for $Sr_xBa_yCo_4Sb_{12}$ at 850 K, respectively.

S.Q. Bai · X.Y. Huang · L.D. Chen (✉) · X.Y. Zhao · Y.F. Zhou
CAS Key Laboratory of Materials for Energy Conversion,
Shanghai Institute of Ceramics, Chinese-Academy of Sciences,
Shanghai 200050, China
e-mail: cld@mail.sic.ac.cn
Fax: 86-21-52413122

W. Zhang
State Key Laboratory of High Performance Ceramics and
Superfine Microstructure, Shanghai Institute of Ceramics,
Chinese Academy of Sciences, Shanghai 200050, China

S.Q. Bai
Graduate University of Chinese Academy of Sciences, Beijing,
China

1 Introduction

Electricity generation using high-efficiency thermoelectric (TE) materials has great potential for applications such as recovery of waste heat [1]. The thermal-to-electricity conversion efficiency of TE material is determined by its figure of merit, $ZT = S^2\sigma T/\kappa$, where S, σ, κ, and T are the Seebeck coefficient, electrical conductivity, total thermal conductivity, and absolute temperature, respectively. Good thermoelectric materials should possess large power factor ($PF = S^2\sigma$) and low thermal conductivity.

Filled skutterudites have been ranked as one of the most promising thermoelectric materials for power generation application and have been intensely pursued for several decades [2]. Various elements from alkaline-earths (Ba, Sr, Ca) [3–5], rare-earths (La, Ce, Yb, Eu, Nd) [6–10], alkaline metals (K, Na) [11, 12], and a few other atoms (Tl, Sn, Ge) [13–15] have been used as filler atoms to fill into the Sb-icosaedron voids in $CoSb_3$ framework. With the relatively high filling fraction limit (FFL) of Ba and effective suppression on lattice thermal conductivity (κ_L), $Ba_yCo_4Sb_{12}$ has been regarded as one of the best n-type TE materials. Due to the close similarity between Ba and Sr, Sr-filled $CoSb_3$ was found to have a high FFL (∼40%) and exhibited good TE performance. A ZT value of 0.9 for $Sr_{0.28}Co_4Sb_{12}$ at 850 K was obtained [4], which is close to that of $Ba_{0.24}Co_4Sb_{12}$ [3]. We also reported the preparation of Sr–Yb double-filled $CoSb_3$, but the pure-phase samples were not obtained due to some unsolved synthesis difficulties at that time [16]. Recently, double-filling has been experimentally proved to be an effective method in depressing κ_L and therefore improving TE performance of filled-skutterudites. The combination of two different type filler atoms with different rattling frequencies, such as one alkaline-earth element and one rare-earth element (AE-RE), has been regarded as the most appreciate choice for double-filled $CoSb_3$ [17]. The high ZT

Table 1 EPMA-measured composition, total thermal conductivity κ, lattice thermal conductivity κ_L, Seebeck coefficient S, electrical conductivity σ, power factor $S^2\sigma$, carrier concentration n, and carrier mobility μ_H at room temperature

EPMA-measured composition	κ (W/m K)	κ_L (W/m K)	S (μV/K)	σ (10^4 S/m)	$S^2\sigma$ (μW cm K^2)	n (10^{20} cm^{-3})	μ_H (cm^2/V s)
$Sr_{0.21}Co_4Sb_{12.25}$	4.9	3.4	−125	24.0	37.8	–	–
$Sr_{0.16}Yb_{0.03}Co_4Sb_{11.82}$	4.1	2.3	−116	29.8	40.3	4.5	37
$Sr_{0.22}Yb_{0.03}Co_4Sb_{12.12}$	4.2	2.2	−109	34.3	41.0	5.3	32
$Sr_{0.11}Ba_{0.18}Co_4Sb_{12.09}$	4.6	2.2	−96	40.1	37.2	–	–

records have been continuously refreshed, for example, 1.26 at 850 K for $Ba_xCe_yCo_4Sb_{12}$ [18] and 1.36 at 850 K for $Ba_xYb_yCo_4Sb_{12}$ [19] have been reported. In dual-element-filled $CoSb_3$, the combinations of Sr with one rare-earth metal (such as Yb) are also expected to be able to depress κ_L effectively and to improve TE performance due to the similar rattling frequency of Sr to that of Ba [17]. However, there is no experimental report on pure-phase double-filled systems with Sr–RE combination. In previous work, the low-temperature transport properties of the $Sr_xBa_yCo_4Sb_{12}$ compounds showed that the AE–AE combination could only weakly depress lattice thermal conductivity [17]. It seems to imply that the combination of two alkaline-earths (AE–AE) has weak effect on the improvement of thermoelectric performance because of the close vibrational frequency of the different alkaline-earths to confirm the conclusion. However, there is no study on high-temperature thermoelectric properties of AE–AE double-filled $CoSb_3$ compounds.

In the present work, we synthesized the single-phase Sr-filled and Sr–Yb, Sr–Ba double-filled $CoSb_3$ samples. The high-temperature thermoelectric properties of these n-type skutterudites are reported. The effects of the different combinations of AE–RE or AE–AE on electrical and thermal transport properties are discussed.

2 Experiment

High-purity metals of Sr (99%, shot), Ba (99%, shot), Yb (99%, piece), Co (99.99%, powder), and Sb (99.9999%, shot) were used as starting materials. The stoichiometric constituent elements were mixed according to the nominal composition $Sr_{0.4}Co_4Sb_{12}$, $Sr_{0.15}Ba_{0.20}Co_4Sb_{12}$, and $Sr_xYb_{0.10}Co_4Sb_{12}$ ($x = 0.2, 0.3$), loaded into carbon crucibles, and then sealed in quartz ampules under vacuum (10^{-3} Pa). The quartz ampules were heated slowly up to 1333–1353 K, soaked for about 4–5 hours, and followed by quenching in a water bath. The resulting ingots were annealed at 1050–1080 K for 168 h and then grounded into fine powders. The powders were loaded into graphite dies and consolidated by a spark plasma sintering (Sumimoto: SPS 2040) process at 863–883 K for 10 minutes under a pressure of 50 MPa.

X-ray diffraction (XRD) and electron microprobe analyses (EPMA) show that all the samples are single phase with the skutterudite structure with trace amount of oxides. The exact compositions of all samples were determined by EPMA. The electrical conductivity (σ) and Seebeck coefficient (S) were measured by the standard four-probe method (ULVAC-RIKO ZEM-3) in He atmosphere between 300 K and 850 K. The carrier concentration (n) and carrier mobility (μ_H) measurements at 300 K were performed in a Quantum Design Physics Property Measurement System (PPMS). The carrier mobility (μ_H) was obtained from the measured electrical conductivity (σ) and carrier concentration (n) by using the expression $\mu_H = \sigma/ne$, where e is the electron charge. The measurements of thermal diffusivity (λ) and specific heat (C_p) were carried out in a flowing Ar atmosphere (Netzsch LFA-427 and DSC 404 C Pegasus, respectively) between 300 K and 850 K. The thermal conductivity (κ) was calculated from the relationship $\kappa = D\lambda C_p$, where D is the mass density. The measured densities of all samples are in the range of 95–99% of the theoretical values. Table 1 list the EPMA-measured composition and room-temperature thermoelectric properties.

3 Result and discussion

Rietveld analysis was employed to refine the crystal structure of $Sr_xYb_yCo_4Sb_{12}$ by using the X-ray powder diffraction (Rigaku D/max 2550V) data in a wide 2θ range (10°–135°). As an example, Fig. 1 shows the observed and calculated XRD patterns and the difference profile between the observed and calculated patterns for $Sr_{0.16}Yb_{0.03}Co_4Sb_{11.82}$. The XRD data of $Sr_{0.16}Yb_{0.03}Co_4Sb_{11.82}$ are refined in space group $Im\bar{3}$ with $a = 9.0669(1)$ Å, $V = 745.399(2)$ Å^3 using RIETAN-2000 [20]. Through reiterative refinement, the reliable factors are $wR_p = 16.18\%$ and $R_p = 12.51\%$. Refined atomic coordinates and thermal parameters for $Sr_{0.16}Yb_{0.03}Co_4Sb_{11.82}$ at room temperature are listed in Table 2. The occupancies of Sr, Yb, and Sb obtained from Rietveld analysis are thus very close to the results from EPMA. It can be seen that the thermal vibration parameters U_{iso} of filling atoms (0.03 for Sr and 0.04 for Yb) are obviously

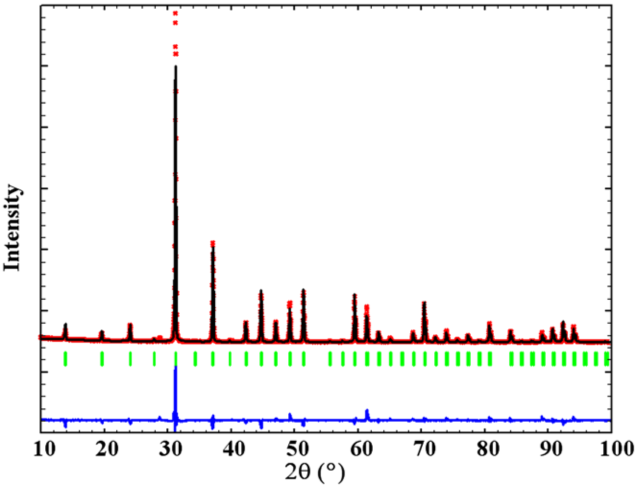

Fig. 1 The XRD refinement for $Sr_{0.16}Yb_{0.03}Co_4Sb_{11.82}$. Dots are the observed intensity, continuous line is the best fit, the difference (obs–calc) is shown at the bottom of the plot along with the tag marks indicating the Bragg positions

Table 2 Refined atomic coordinates and thermal parameters for $Sr_{0.16}Yb_{0.03}Co_4Sb_{11.82}$ at room temperature. The refined lattice parameter a is 9.0669(1) Å

Atom	Site	x	y	z	U_{iso}	Occu.
Co1	8c	0.25	0.25	0.25	0.0077(8)	1
Sb1	24g	0	0.3352(1)	0.1582(1)	0.0046(2)	1
Sr1	2a	0	0	0	0.038(6)	0.16
Yb1	2a	0	0	0	0.039(6)	0.03

larger than those of frame atoms (0.007 for Co and 0.004 for Sb). This result is similar to the previous work [21, 22]. The relatively large U_{iso} of the filling atoms indicate that the bonding between the filling atoms and their adjacent atoms is loose. Consequently, the filling atoms can rattle inside the oversized Sb-icosahedron voids and lead to the reduction of lattice thermal conductivity.

Figure 2 shows the temperature dependence of electrical conductivity (σ) and Seebeck coefficient (S) for all samples. The electrical conductivity (σ) decreases, and the absolute value of Seebeck coefficient (S) increases with increasing temperature. With increasing total filling fraction ($x + y$), σ increases, and S decreases in the whole temperature range, which shows a typical behavior of heavily doped semiconductors. Figure 3 shows the temperature-dependent power factor ($S^2\sigma$) for all samples. With increasing temperature, the power factors of the $Sr_xYb_yCo_4Sb_{12}$ are much greater as compared with those of the single-element-filled $Sr_{0.21}Co_4Sb_{12.25}$ skutterudite. The maximum power factor for double-filled $CoSb_3$ systems reaches 57.5 µW cm^{-1} K^{-2} at 850 K, which is about 20% high than Sr single-filled one. The increasing in the power factor for Sr–Yb filled skutterudites may be caused by the effective mass elevation.

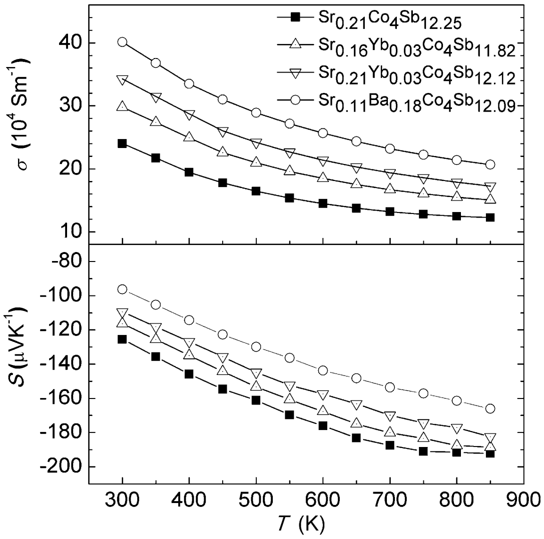

Fig. 2 Measured temperature dependence of the electrical conductivity (σ) and Seebeck coefficient (S) for $Sr_{0.21}Co_4Sb_{12.25}$ (*filled squares*), $Sr_xYb_yCo_4Sb_{12}$ (*open triangles*), and $Sr_xBa_yCo_4Sb_{12}$ (*open circles*)

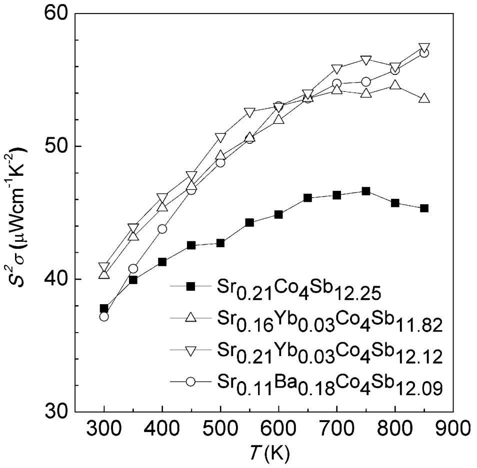

Fig. 3 Measured temperature dependence of power factor ($S^2\sigma$) for $Sr_{0.21}Co_4Sb_{12.25}$ (*filled squares*), $Sr_xYb_yCo_4Sb_{12}$ (*open triangles*), and $Sr_xBa_yCo_4Sb_{12}$ (*open circles*)

Figure 4 shows the effective mass as a function of carrier concentration for Sr- [4] and Ba-single-element-filled $CoSb_3$ [3, 24], $Ba_xCe_yCo_4Sb_{12}$ (from Ref. [18]) and $Sr_xYb_yCo_4Sb_{12}$ double-filled $CoSb_3$ compounds at 300 K. Our recent work on $Ba_xCe_yCo_4Sb_{12}$ double-filled skutterudites showed that the electrical transport properties in the dual-element-filled and single-element-filled $CoSb_3$ skutterudites have similar tendency regarding to their scattering mechanism and carrier concentration dependency [18]. The low-temperature carrier mobility measurements indicated that the electrons are mainly scattered by acoustic lattice phonons in $Sr_xYb_yCo_4Sb_{12}$. Therefore the relaxation time could be expressed as $\tau_L = \tau_{0L}E^{-1/2}$, where E is the re-

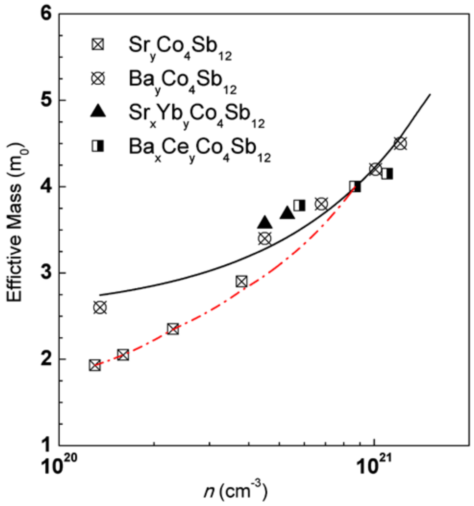

Fig. 4 Calculated effective mass as a function of carrier concentration for $Sr_yCo_4Sb_{12}$ [3], $Ba_yCo_4Sb_{12}$ [22], $Ba_xCe_yCo_4Sb_{12}$, and $Sr_xYb_yCo_4Sb_{12}$ double-filled ones at 300 K. The *solid line* is the best fit to the data for $Ba_yCo_4Sb_{12}$. The *dash line* is the best fit to the data for $Sr_yCo_4Sb_{12}$

duced carrier energy. Within single parabolic band approximation, the relevant Seebeck coefficient and carrier concentration in the relaxation time approximation for acoustic phonon scattering are

$$S = \pm\frac{k_B}{e}\left(\frac{(r+\frac{5}{2})F_{r+3/2}(\eta)}{(r+\frac{3}{2})F_{r+1/2}(\eta)} - \eta\right) \qquad (1)$$

and

$$n = 4\pi\left(\frac{2m^*k_BT}{h^2}\right)^{3/2}F_{1/2}(\eta), \qquad (2)$$

where k_B is the Boltzmann constant, h is the Planck constant, $F_r(\eta)$ are the Fermi integrals of order r (for acoustic phonon scattering, $r = -1/2$), e is the electron charge, and $\eta = E_F/k_BT$, where E_F is the Fermi level. The effective masses are calculated using (1) and (2). The solid and dot lines in Fig. 4 are the fit lines for $Ba_yCo_4Sb_{12}$ [3, 23] and $Sr_yCo_4Sb_{12}$ [4] data to the Kane model, respectively. The Sr and Yb cofilling leads to an elevation in effective mass, resulting in the increasing of power factor, as compared to Sr-single-filled $CoSb_3$. Recently, Yang et al. found that an optimized doping level is 0.5 electrons per unit cell for maximizing power factors of n-type filled $CoSb_3$ compounds [24]. For $Sr_{0.22}Yb_{0.03}Co_4Sb_{12.12}$, both Sr and Yb offer two electrons to $CoSb_3$ matrix, the doping level is close to 0.5 electrons per unit cell, and its power factor almost reaches a value as high as 58 $\mu W\,cm^{-1}\,K^{-2}$ at 850 K. This result agrees well with Yang's conclusion.

Figure 5 plots the temperature dependence of the measured total thermal conductivity (κ) and the estimated lattice thermal conductivity ($\kappa_L = \kappa - \kappa_e$) for all samples.

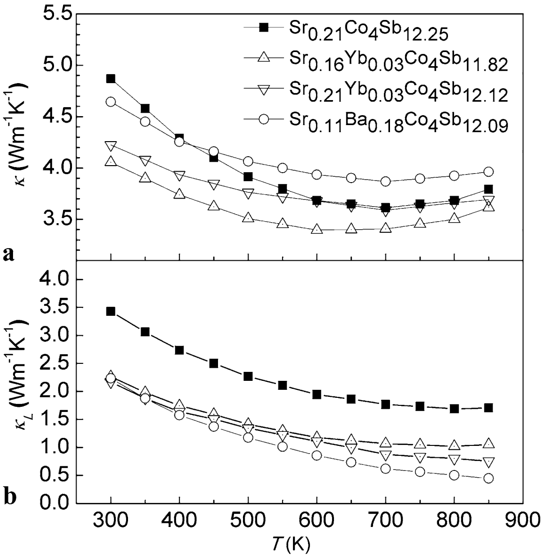

Fig. 5 (**a**) Measured temperature dependence of total thermal conductivity (κ) for Sr-single-filled skutterudites (*filled squares*), $Sr_xYb_yCo_4Sb_{12}$ (*open triangles*), and $Sr_xBa_yCo_4Sb_{12}$ double-filled ones (*open circles*); (**b**) Calculated lattice thermal conductivity (κ_L) for Sr-single-filled skutterudites (*filled squares*), $Sr_xYb_yCo_4Sb_{12}$ (*open triangles*), and $Sr_xBa_yCo_4Sb_{12}$ double-filled ones (*open circles*)

The electron thermal conductivity (κ_e) is estimated by using the Wiedemann–Franz law $\kappa_e = L_0T\sigma$, where the Lorenz number L_0 has a value of 2.0×10^{-8} $V^2\,K^{-2}$ based on the estimation of by Dyck et al. for $Ba_yCo_4Sb_{12}$ compounds [23]. As compared with Sr single-element-filled compounds, the lattice thermal conductivities of the Sr–Yb double-filled $CoSb_3$ compounds drop about 40% in the whole temperature range, indicating that the Sr–Yb cofilling effectively suppresses κ_L of $CoSb_3$. This result is similar to our previous work on Ba–Ce double-filled $CoSb_3$ compounds. Figure 6 shows the room-temperature lattice thermal resistivity ($W_L = 1/\kappa_L$) as a function of filling fraction y for ($Sr_yCo_4Sb_{12}$) [4] or total filling fraction $x + y$ ($Sr_xYb_yCo_4Sb_{12}$, $Sr_xBa_yCo_4Sb_{12}$, and $Ba_xCe_yCo_4Sb_{12}$) [18]. The room-temperature lattice thermal resistivities of $Sr_yCo_4Sb_{12}$ compounds exhibit a liner relationship with filling fraction y. Cofilling using combination of different types of filler atoms could significantly increase the lattice thermal resistivity of the $Sr_xYb_yCo_4Sb_{12}$ and $Ba_xCe_yCo_4Sb_{12}$ compounds. At similar total filling fraction, double-filled $CoSb_3$ with AE–RE combination has a much higher W_L than that of $Sr_yCo_4Sb_{12}$. For AE–AE cofilling, the effect on suppression κ_L using the combination of Sr and Ba is a little weaker than that of using the combination of different type fillers, such as AE–RE.

Figure 7(a) shows the calculated dimensionless thermoelectric figure of merit as a function of temperature. The ZT value of $Sr_{0.21}Co_4Sb_{12.25}$ achieves 1.0 at 850 K. The n-type $Sr_xYb_yCo_4Sb_{12}$ and $Sr_xBa_yCo_4Sb_{12}$ compounds show enhanced ZT values as compared to $Sr_{0.21}Co_4Sb_{12.25}$ in the

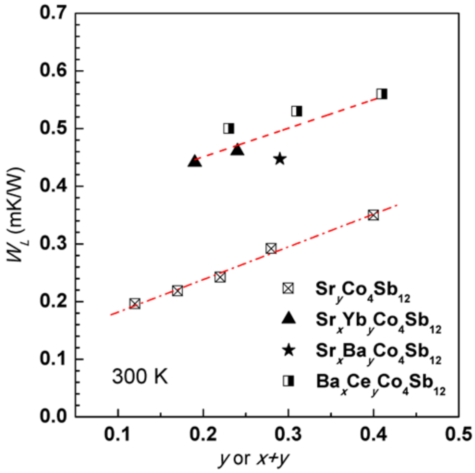

Fig. 6 Lattice thermal resistivity (W_L) as a function of filling fraction (y) for $Sr_yCo_4Sb_{12}$ [3] and total filling fraction ($x + y$) for $Sr_xYb_yCo_4Sb_{12}$, $Sr_xBa_yCo_4Sb_{12}$, and $Ba_xCe_yCo_4Sb_{12}$ [17] at 300 K. The *dot lines* are the guides to the eye

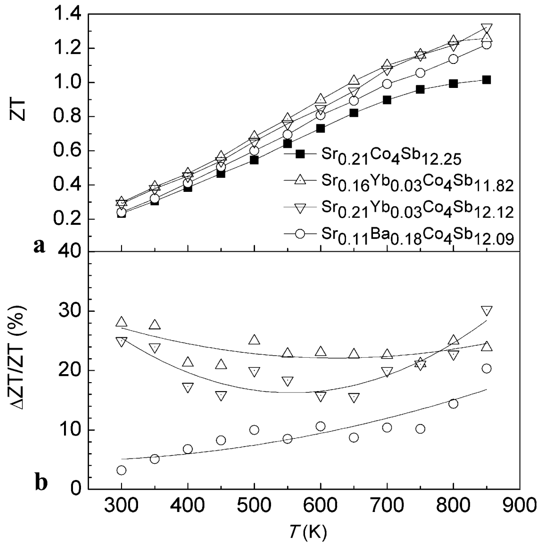

Fig. 7 (**a**) Temperature-dependent dimensionless figure of merit (ZT) for $Sr_{0.21}Co_4Sb_{12.25}$ (*filled squares*), $Sr_xYb_yCo_4Sb_{12}$ (*open triangles*), and $Sr_xBa_yCo_4Sb_{12}$ (*open circles*). (**b**) Temperature dependence of $\Delta ZT/ZT$ ratio for $Sr_xYb_yCo_4Sb_{12}$ (*open triangles*) and $Sr_xBa_yCo_4Sb_{12}$ (*open circles*) as compared with the ZT value of $Sr_{0.21}Co_4Sb_{12}$. The *solid lines* are the guides to the eye

entire temperature range studied. The ZT values reaches 1.32 at 850 K for $Sr_{0.22}Yb_{0.03}Co_4Sb_{12.12}$ comparable to the best value of 1.36 for n-type Ba–Yb double-filled $CoSb_3$ compounds [19]. In the whole temperature range, the ZT values for $Sr_xYb_yCo_4Sb_{12}$ compounds are 20–30% higher than that of $Sr_{0.21}Co_4Sb_{12.25}$, as shown in Fig. 7(b). Meanwhile, for Sr–Ba system, the cofilling using the combination of same type of alkaline-earth atoms only causes 10–20% enhancement in ZT value. A ZT value of 1.22 is obtained for $Sr_{0.11}Ba_{0.18}Co_4Sb_{12.09}$ at 850 K.

4 Conclusion

Single-phase polycrystalline dual-element-filled skutterudites $Sr_xYb_yCo_4Sb_{12}$ and $Sr_xBa_yCo_4Sb_{12}$ were synthesized. Sr–Yb cofilling leads to a much stronger reduction in lattice thermal conductivity (κ_L) than Sr–Ba cofilling, proving again that the combinations of different types of filler atoms are more effective on κ_L suppression than the combinations of same types of fillers. The enhanced thermoelectric performance is realized in the double-filled $CoSb_3$ systems. The ZT value reaches 1.32 (850 K) for $Sr_{0.16}Yb_{0.03}Co_4Sb_{11.82}$ and 1.22 (850 K) for $Sr_{0.11}Ba_{0.18}Co_4Sb_{12.09}$, respectively. Furthermore, the ZT enhancements in the whole temperature range are obtained. Further compositional optimization is expected to lead to even higher ZT for the Sr–Yb cofilled $CoSb_3$. The concept of enhancing thermoelectric figure of merit ZT by multiple filling should also be effective for other caged compounds, such as clathrates.

Acknowledgements This work is supported in part by National Basic Research Program of China (973 program) under Project Nos. 2007CB607503 and 2007CB607502, NSFC projects (50821004, 50820145203, and 50825205), and the Science and Technology Commission of Shanghai Municipality No. 08DZ2210900.

References

1. G.A. Slack, in *CRC Handbook of Thermoelectrics*, ed. by D.M. Rowe (CRC, Boca Raton, 1995), p. 407
2. B.C. Sales, D. Mandrus, R.K. Williams, Science **272**, 1352 (1996)
3. L.D. Chen, T. Kawahara, X.F. Tang, T. Goto, T. Hirai, J.S. Dyck, W. Chen, C. Uher, J. Appl. Phys. **90**, 1864 (2001)
4. X.Y. Zhao, X. Shi, L.D. Chen, W.Q. Zhang, W.B. Zhang, Y.Z. Pei, J. Appl. Phys. **99**, 053711 (2006)
5. M. Puyet, B. Lenoir, A. Dauscher, M. Dehmas, C. Stiewe, E. Műller, J. Appl. Phys. **95**, 4852 (2004)
6. G.S. Nolas, J.L. Cohn, G.A. Slack, Phys. Rev. B **58**, 164 (1998)
7. D.T. Morelli, G.P. Meisner, B.X. Chen, S.Q. Hu, C. Uher, Phys. Rev. B **56**, 7376 (1997)
8. G.S. Nolas, M. Kaeser, R.T. Littleton IV, T.M. Tritt, Appl. Phys. Lett. **77**, 1855 (2000)
9. G.A. Lamberton Jr., S. Bhattacharya, R.T. Littleton IV, M.A. Kaeser, R.H. Tedstrom, T.M. Tritt, J. Yang, G.S. Nolas, Appl. Phys. Lett. **80**, 598 (2002)
10. V.L. Kuznetsov, L.A. Kuznetsova, D.M. Rowe, J. Phys., Condens. Matter **15**, 5035 (2003)
11. Y.Z. Pei, L.D. Chen, W. Zhang, X. Shi, S.Q. Bai, X.Y. Zhao, Z.G. Mei, X.Y. Li, Appl. Phys. Lett. **89**, 221107 (2006)
12. Y.Z. Pei, J. Yang, L.D. Chen, W. Zhang, J.R. Salvador, J. Yang, Appl. Phys. Lett. **95**, 042101 (2009)
13. B.C. Sales, B.C. Chakoumakos, D. Mandrus, Phys. Rev. B **61**, 2475 (2000)
14. G.S. Nolas, H. Takizawa, E. Endo, H. Sellinschegg, D.C. Johnson, Appl. Phys. Lett. **77**, 52 (2000)
15. G.S. Nolas, J. Yang, H. Takizawa, Appl. Phys. Lett. **84**, 5210 (2004)
16. S.Q. Bai, X.Y. Zhao, Y.Z. Pei, L.D. Chen, W.Q. Zhang, in *Proceedings of the 25th International Conference of Thermoelectrics*, Vienna, Austria, 6–10 August 2006. doi:10.1109/ICT.2006.331301

17. J. Yang, W. Zhang, S.Q. Bai, Z. Mei, L.D. Chen, Appl. Phys. Lett. **90**, 192111 (2007), and references therein
18. S.Q. Bai, Y.Z. Pei, L.D. Chen, W.Q. Zhang, X.Y. Zhao, J. Yang, Acta Mater. **57**, 3135 (2009)
19. X. Shi, H. Kong, C.P. Li, C. Uher, J. Yang, J.R. Salvador, H. Wang, L. Chen, W. Zhang, Appl. Phys. Lett. **92**, 182101 (2008)
20. F. Izumi, T. Ikeda, Mater. Sci. Forum **321–324**, 198 (2000)
21. X.F. Tang, H. Li, Q.J. Zhang, M. Niino, T. Goto, J. Appl. Phys. **100**, 123702 (2006)
22. W.Y. Zhao, C.L. Dong, P. Wei, W. Guan, L.S. Liu, P.C. Zhai, X.F. Tang, Q.J. Zhang, J. Appl. Phys. **102**, 113708 (2007)
23. J.S. Dyck, W. Chen, C. Uher, L.D. Chen, X.F. Tang, T. Hirai, J. Appl. Phys. **91**, 3698 (2002), and references therein
24. J. Yang, L. Xi, W. Zhang, L.D. Chen, J.H. Yang, J. Electron. Mater. (2009). doi:10.1007/s11664-009-07030-9